ENGINEERING TRANSACTIONS • *Engng. Trans.* • **44**, 2, 181–206, 1996
Polish Academy of Sciences • Institute of Fundamental Technological Research

INFLUENCE OF CONSTANT AND MONOTONIC LOADINGS ON SUBSEQUENT BIAXIAL BEHAVIOUR OF 15 HM BOILER STEEL

Z. L. KOWALEWSKI (WARSZAWA)

Experimental analysis is presented of the plastic properties of 15 HM boiler steel in the as-received state and of the same material subjected to various types of predeformation. The analysis was made by studying the positions in the stress space and typical dimensions of the yield surfaces. The initial yield surface has been determined using the technique of sequential probes of the single specimen and this surface was used as the starting point for comparative studies of yield surfaces of the prestrained material. The material predeformations were induced either by a creep process or by monotonic loading, both at ambient temperature. After predeformation, yield surfaces were determined by the same method as that for the non-prestrained material. The anisotropic yield condition was used to create a least squares fit of the experimental results. Prior cold work induced the weakening effect of the steel in the considered plastic strain range. The material tested after prestraining, independently of the predeformation type, exhibited the Bauschinger effect.

1. Introduction

The effect of plastic prestrain induced in metals during either manufacturing processes of semi-finished elements or during exploitation of structural components is a problem being intensively studied by a number of research centers [1–39]. Direct reason of such great interest in this problem results from different responses of various materials subjected to the same type of predeformation. For some materials plastic prestraining can cause a hardening effect [2, 4, 7, 9–14, 19, 21–23], for the others, however, a weakening effect can be observed [3, 20, 38, 39]. It has been also shown that in certain cases, cold work has no influence on subsequent material behaviour [6]. Generally, all investigations concerning the influence of predeformation on the basic material parameters can be classified into the following categories:

A. Investigations with predeformation induced due to monotonic loading of a testpiece, e.g. [11, 13, 20, 24].

B. Investigations with predeformation induced due to cyclic loading of a testpiece, e.g. [15–18, 20, 21].

C. Investigations with predeformation induced due to creep process of a testpiece tested at room or elevated temperatures, e.g. [11, 26–29].

Results of these investigations are especially important for some industrial branches, such as aircraft, chemical industry, power plants, etc. Since in the mentioned branches an extreme care is taken on the safety conditions, there is the greatest demand for experiments giving information concerning material properties after either plastic predeformation during forming processes, or heat treatment for wider group of materials. The results available in scientific papers are still insufficient, since they have been obtained mainly at uni-axial tests and, moreover, they cover a narrow group of engineering materials.

All investigations giving the accurate data concerning material properties have to be performed at multiaxial stress states. The number of these tests are limited because of both their extremely high cost and the difficulties in strain measurements, and, as a consequence, it often leads to difficulties in comparative studies of experimental results obtained from such investigations. Results from experiments carried out at complex stress states are usually presented in the form of a yield surface cross-section which is connected with the stress state realized in the testpiece. Unfortunately, due to

- variations in stress states considered by different investigators,
- differences in accuracy of strain measurement,
- differences in the definition of yield limit, and
- influence of loading conditions and the resulting disturbations in the stress state homogeneity on the gauge length of the specimen,

in such a form of data analysis, great difficulties appear in their reliable interpretation. Therefore, in order to ensure a comparison of the results of experiments carried out in different labs, it is necessary to determine accurately all boundary conditions of tests.

The paper presents the results of multiaxial tests. The main aim of the experimental programme was to determine the shape and dimensions of an initial yield surface of 15 HM boiler steel and its evolution due to different forms of plastic predeformation. The material was chosen because of its common applicability in numerous engineering components.

2. Experimental procedure

2.1. Material, testpiece and testing equipment

Tests have been carried out with the use of 15 HM boiler steel in the as-received state. The chemical composition of the material is given in Table 1. It can be applied at high temperatures and typically is used in such en-

gineering structures as vapour and water boilers, pressure vessels, pipelines, etc. It is most often provided in form of sheets, tubes, rods and forgings.

Table 1. Chemical composition of 15 HM boiler steel.

	C	Mn	Si	P_{max}	S_{max}	Cr	Ni_{max}	Mo	Cu	Al_{max}
	[%]	[%]	[%]	[%]	[%]	[%]	[%]	[%]	[%]	[%]
15 HM	0.11÷0.18	0.4÷0.7	0.15÷0.35	0.04	0.04	0.7÷1.0	0.35	0.4÷0.55	>0.25	0.02

Specimens were manufactured from tubes of 44 [mm] external diameter and 36 [mm] internal diameter. An engineering drawing of the specimen is shown in Fig. 1.

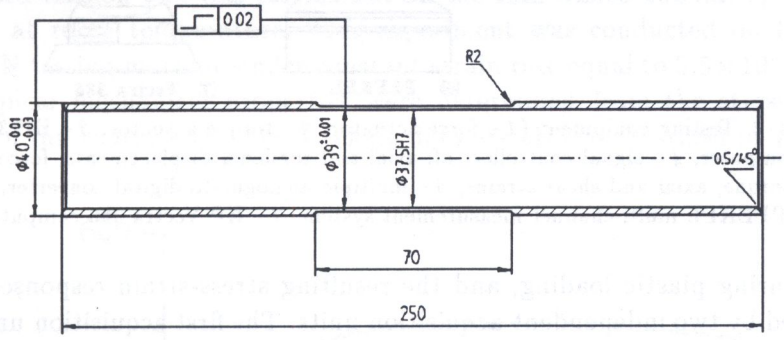

FIG. 1. Testpiece.

All experiments reported in this paper were carried out with the use of the MODEL 1343 INSTRON (shown in Fig. 2) electrohydraulic, closed-loop, servo-controlled, biaxial testing machine enabling combined loading in tension – compression – torsion – reverse torsion. The maximum axial and torsional load capacities are rated at ±100 [kN] and ±1000 [Nm], respectively. Two separate servo-controller units connected to a HP 310 computer of the INSTRON loading system can independently apply controlled axial loads and torsional moments. The hydraulic pressure in the actuators comes from two servo-valves operated by servo-controllers provided with set-point control signals from the computer. A multiple analogue-to-digital converter feeds the HP310 computer with the signals of axial displacement of machine piston, rotation of the grip fixture of a specimen, axial force, twisting moment, axial strain and torsional strain.

The axial force and the torque applied to the specimen were measured using load cells incorporated in the machine. The software which was specially developed for these tests enabled the maintenance of constant effective strain

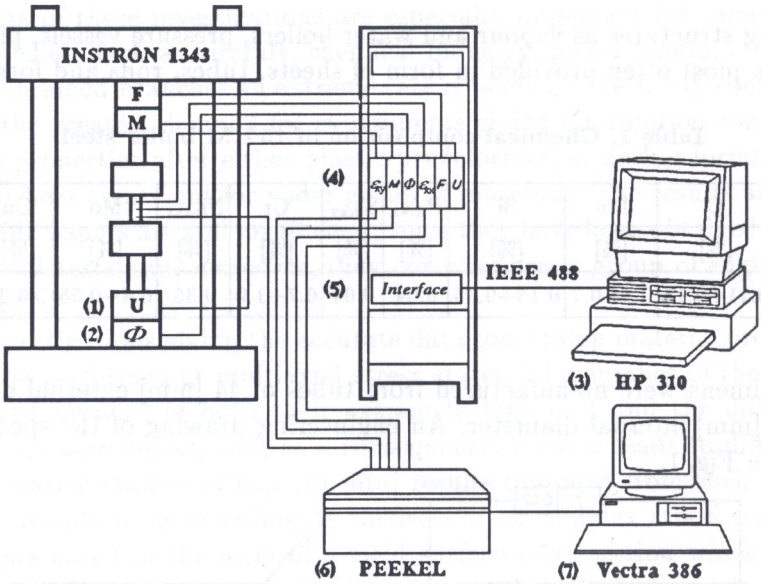

FIG. 2. Testing equipment (*1* – force actuator, *2* – torque actuator, *3* – HP 310 computer, *4* – signal controllers of: axial and torsional displacements, force, torque, axial and shear strains, *5* – multiple analogue-to-digital converter, *6* – PEEKEL multi-channel measurement system, *7* – HP Vectra 386 computer).

rates during plastic loading, and the resulting stress-strain responses were recorded by two independent acquisition units. The first acquisition unit was connected to the HP 310 control computer and, for this reason, had a rather limited ability to display current progress of an experiment. The second acquisition unit operated independently of the control computer. It mainly comprised a PEEKEL multi-channel measurement system from which the signals were fedback to a Hewlett-Packard Vectra 386 computer, thus enabling both direct on-line observations of the experimental results and also their saving onto the hard disk of the computer during each test.

2.2. Strain measurement

The strains were measured using the foil strain gauges bonded to the outer surface of the specimen. Axial strains were measured by a full bridge circuit of four strain gauges of which two, located on the opposite sides of the specimen gauge length were active, while the other two, located on a specially designed semi-ring, were used for temperature compensation. The shear strains circuit also contained a full bridge of four strain gauges. They were bonded to the specimen surface inclined at 45° to the specimen

axis. Both these strain measurement circuits were connected to both the INSTRON and the PEEKEL measurement systems. At all tests, the hoop strains were also registered by means of the half bridge circuit of two strain gauges connected to the PEEKEL measurement system. Before the test run, both these circuits were calibrated using a highly sensitive Hottinger tensometric bridge (UGR 60) so that the 0.8 [%] strain value was set to correspond to the maximum control signal of 10 [V].

2.3. Preliminary investigations of the basic mechanical parameters

In order to determine mechanical properties of the tested material, the standard tension test was carried out on the thin-walled tubular specimen, Fig. 1, at room temperature. This experiment was conducted on the INSTRON testing machine under constant strain rate equal to 3.5×10^{-4} [1/s]. All typical mechanical properties were determined from the stress-strain curve of the 15 HM steel, Fig. 3. These data are also summarized in Table 2.

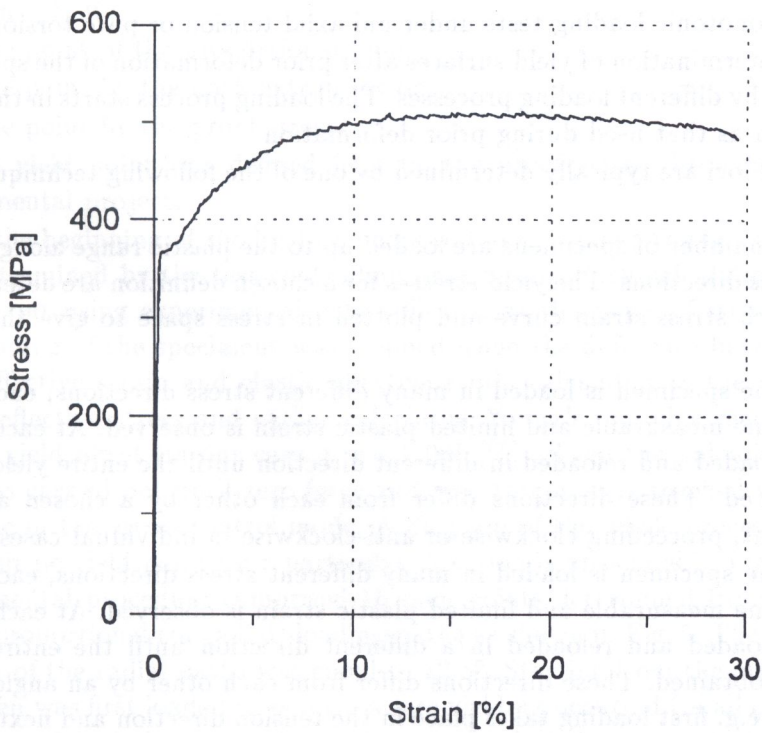

FIG. 3. Monotonic tension stress-strain curve of the 15 HM boiler steel.

Table 2. Mechanical properties of tested 15 HM boiler steel.

Mechanical properties at room temperature	Value
Young's modulus E	2.2×10^5 [N/mm^2]
upper yield limit	375 [N/mm^2]
lower yield limit	370 [N/mm^2]
ultimate tensile stress R_m	510 [N/mm^2]
elongation	29 [%]

2.4. Description of the investigation programme

The experimental programme comprised the following steps:

1. Determination of an initial yield surface using the sequential loading of a single specimen for the sixteen different loading paths equally distributed in all quadrants of the (σ_{xx}, τ_{xy}) plane. The loading process starts in the uni-axial tension direction.

2. Prior deformation of the specimens; it was realized by:

a) biaxial creep tests under constant effective stress level,

b) monotonic loading tests under uni-axial tension or pure torsion.

3. Determination of yield surfaces after prior deformation of the specimen induced by different loading processes. The loading process starts in the same direction as that used during prior deformation.

Yield loci are typically determined by one of the following techniques [14, 24, 30]:

a. A number of specimens are loaded up to the plastic range along different stress directions. The yield stresses for a chosen definition are determined from each stress-strain curve and plotted in stress space to give the yield locus.

b. One specimen is loaded in many different stress directions, each time until some measurable and limited plastic strain is observed. At each point it is unloaded and reloaded in different direction until the entire yield locus is obtained. These directions differ from each other by a chosen angular increment, proceeding clockwise or anti-clockwise in individual cases.

c. One specimen is loaded in many different stress directions, each time until some measurable and limited plastic strain is observed. At each point it is unloaded and reloaded in a different direction until the entire yield locus is obtained. These directions differ from each other by an angle equal to 180°, e.g. first loading takes place in the tension direction and next in the compression direction, etc.

According to previous experiments, the first method gives results which are qualitatively best, since in this case the shape of the yield surface is not disturbed by the history of the previous probes performed on the same specimen in order to determine the other points of the yield locus. It has been found [43], however, that under certain conditions either b) or c) single-specimen methods can be successfully applied to the yield surface determination. In these methods small plastic strains are needed to define yielding and they have to use a specific sequence of loading which should be the same for the whole experimental procedure. Moreover, the use of single-specimen methods overcomes the disadvantages of the first method, such as having to use a number of expensive specimens to determine each yield locus, and also having to deal with errors due to possible specimen-to-specimen variations. These effects have been previously studied in detail by a number of researchers [14, 24, 30]. Taking into account these considerations, the single specimen method described in point b) has been adopted for the yield surface determination.

The definition of the yield point may have a remarkable effect on the resulting shape and dimensions of the yield surface. Generally, the yield point is defined by one of the following three points in the stress-strain diagram [14, 30]:

- the point of the proportional limit,
- the point by the back extrapolation,
- the point by the proof stress.

The yield point was defined here by the proof stress throughout this experimental project.

At the beginning of the loading phase of the specimen, Young's modulus was determined by the test controlling programme. Such calculations were carried out using experimental data collected at the range of stress levels. The loading of the specimens was stopped when the difference between the total effective strain and elastic effective strain calculated as the quotient of the effective stress and earlier calculated Young's modulus reached the chosen yield offset (in our case it was 0.005 [%]). Then the unloading process was carried out until zero force and zero torque were reached with the machine in the stress control mode. A diagram of the whole process to obtain a single yield point for a particular direction is presented in Fig. 4. The experimental procedure comprised 16 such points determined from the selected proportional (or radial) loading paths as shown in Fig. 5. The angular spacing of the radial paths was equal to 22.5°. Starting from the origin, the specimen was first loaded to point 1 where yielding occurred (in all cases the loading path including point 1 was the same as direction of prestraining), as

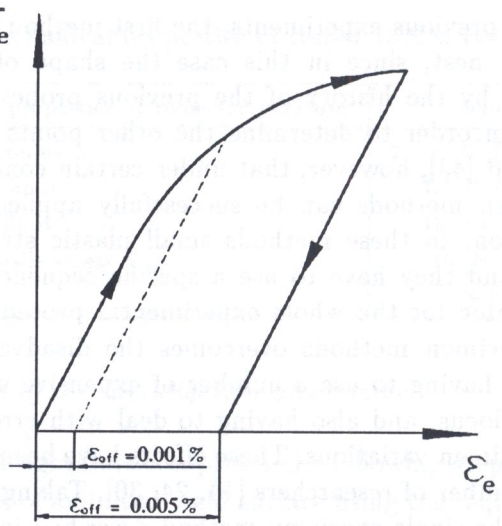

FIG. 4. Scheme of the loading process used to determine a single point of the yield surface.

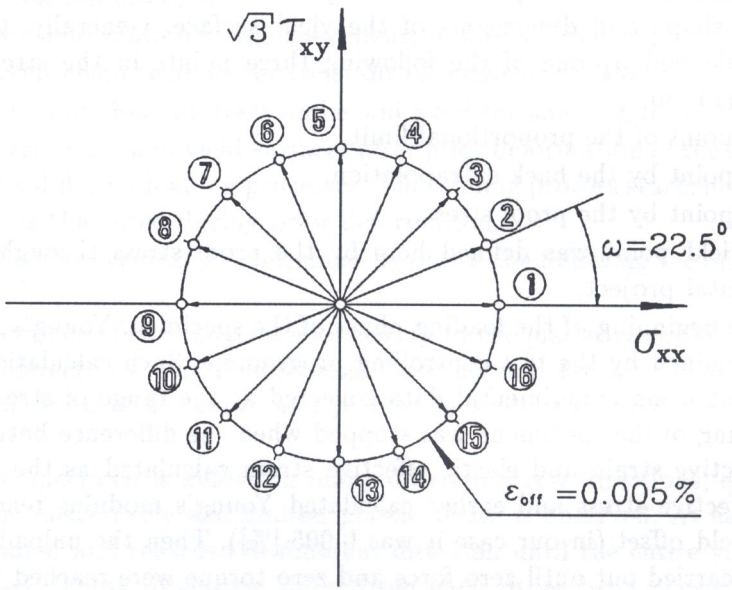

FIG. 5. Loading sequence for yield locus determination.

defined above, and then the specimen was completely unloaded and again loaded in the subsequent direction up to point 2 where again yielding occurred. The sequence so described was repeated until all 16 yield points were determined. In Fig. 5 the increasing numbers at the yield points indicate the loading sequence.

In the second part of the experimental procedure creep prestrain tests as well as monotonic loading tests were performed on the Instron testing machine at room temperature. The creep process was carried out for the three types of loading combinations, Fig. 6, (uni-axial tension, combination of tension and torsion, and pure torsion), required to give in plane stress state the same effective stress level equal to 370 [MPa]. All creep tests were conducted for two hours and then stopped by immediate unloading of the testpiece.

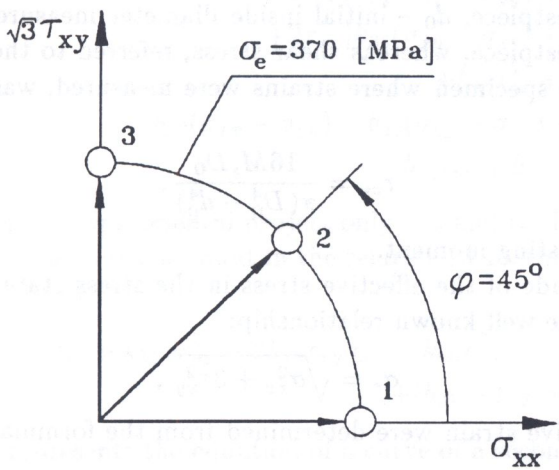

FIG. 6. Programme of creep tests.

The stage 2*b* of the testing project comprised investigations during which prior deformations were induced by standard monotonic tension or torsion tests. These tests were carried out up to the same magnitudes of total effective plastic prestrain equal to 0.65 [%]. The loading process was being automatically stopped when the prescribed amount of plastic predeformation was achieved. At this time the strain control mode of the testing machine was being changed to the stress control mode and the unloading process was carried out until zero force and zero torque were reached.

When prestraining process of each specimen was completed, the determination of the yield surface was performed on the INSTRON testing machine with the use of the same procedure as that previously applied for the non-prestrained material. For the prestrained material the first probe of the yield surface determination procedure was always carried in the direction which was coincident with the predeformation path. Directions of the subsequent probes were changed anti-clockwise by the angular increment assumed to be 22.5°.

2.5. Relationships defining stress and strain

The stress state components were defined with regard to the initial specimen dimensions by the commonly used relations for thin-walled tubes. Namely, axial stress was expressed by the following formula:

$$\sigma_{xx} = \frac{4F}{\pi(D_0^2 - d_0^2)}, \tag{2.1}$$

where F – axial force, D_0 – initial outside diameter measured within gauge length of the testpiece, d_0 – initial inside diameter measured within gauge length of the testpiece, whereas shear stress, referred to the initial outside diameter of the specimen where strains were measured, was defined in the form:

$$\tau_{xy} = \frac{16M_s D_0}{\pi(D_0^4 - d_0^4)}, \tag{2.2}$$

where M_s – twisting moment.

The magnitude of the effective stress in the stress state considered was expressed by the well known relationship:

$$\sigma_e = \sqrt{\sigma_{xx}^2 + 3\tau_{xy}^2}, \tag{2.3}$$

while the effective strain were determined from the formula involving Poisson's ratio ν:

$$\varepsilon_e = \sqrt{\varepsilon_{xx}^2 + \frac{3}{(1+\nu)^2}\varepsilon_{xy}^2}, \tag{2.4'}$$

where ε_{xx} – axial strain, $\varepsilon_{xy} = \gamma_{xy}/2$ – shear strain.

When $\nu = 0.5$, then this equation simplifies to the form:

$$\varepsilon_e = \sqrt{\varepsilon_{xx}^2 + \frac{1}{3}\gamma_{xy}^2}. \tag{2.4''}$$

The experimentally determined Poisson's ratio ν for the steel tested was equal to 0.34. Thus, Eq. (2.4') was used in all calculations of the effective strain.

3. Yield condition

Yield locus can be represented in a stress space by the experimental points determined on the basis of stress-strain diagrams for the magnitude of the effective stress assumed as a yield definition. These points determine the shape, dimensions and location of the yield surface.

The MISES anisotropic yield condition [42] in the form derived by SZCZEPIŃSKI [37] has been adopted in numerical calculations. It reflects both the Bauschinger effect representing a shift of yield surface axes with respect to the origin of the coordinate system applied, and a rotation of the yield locus axes. Generally, it can be expressed by the following relationship

$$
\begin{aligned}
(3.1)\qquad f(\sigma_{ij}) = {} & k_{12}(\sigma_{xx}-\sigma_{yy})^2 + k_{23}(\sigma_{yy}-\sigma_{zz})^2 + k_{31}(\sigma_{zz}-\sigma_{xx})^2 \\
& + 2\tau_{xy}\,[k_{16}(\sigma_{zz}-\sigma_{xx}) + k_{26}(\sigma_{zz}-\sigma_{yy})] \\
& + 2\tau_{yz}\,[k_{24}(\sigma_{xx}-\sigma_{yy}) + k_{34}(\sigma_{xx}-\sigma_{zz})] \\
& + 2\tau_{zx}\,[k_{35}(\sigma_{yy}-\sigma_{zz}) + k_{15}(\sigma_{yy}-\sigma_{xx})] \\
& + k_{44}\tau_{yz}^2 + k_{55}\tau_{zx}^2 + k_{66}\tau_{xy}^2 \\
& - b_{12}(\sigma_{xx}-\sigma_{yy}) - b_{23}(\sigma_{yy}-\sigma_{zz}) - b_{31}(\sigma_{zz}-\sigma_{xx}) \\
& + b_{44}\tau_{yz} + b_{55}\tau_{zx} + b_{66}\tau_{xy} = 1.
\end{aligned}
$$

In the tests of our experimental project only σ_{xx} and τ_{xy} had nonzero values. When this is taken into account in the relation (3.1), the yield condition is simplified as follows:

$$
\begin{aligned}
(3.2)\qquad f(\sigma_{ij}) = {} & (k_{12}+k_{31})\sigma_{xx}^2 - 2k_{16}\tau_{xy}\sigma_{xx} + k_{66}\tau_{xy}^2 \\
& + (b_{31}-b_{12})\sigma_{xx} + b_{66}\tau_{xy} = 1.
\end{aligned}
$$

This expression represents the equation of a curve of a second order, usually written in the form:

$$
(3.3)\qquad A\sigma_{xx}^2 + 2B\sigma_{xx}\tau_{xy} + C\tau_{xy}^2 + 2D\sigma_{xx} + 2F\tau_{xy} = 1,
$$

where coefficients A and D are related to the yield limits determined from tests under tension and compression, respectively. They can be expressed as follows:

$$
(3.4)\qquad A = \frac{1}{Y_{xx}Z_{xx}}, \qquad 2D = \frac{1}{Y_{xx}} - \frac{1}{Z_{xx}},
$$

where Y_{xx} and Z_{xx} are the yield limits for tension and for compression, respectively.

The coefficients C and F are related to the shear yield limits obtained from tests under torsion and reverse torsion, respectively. They can be written in the following simple form:

$$
(3.5)\qquad C = \frac{1}{R_{xy}S_{xy}}, \qquad 2F = \frac{1}{R_{xy}} - \frac{1}{S_{xy}},
$$

where R_{xy} denotes the yield limit obtained under positive shear stress and S_{xy} denotes the yield limit obtained under negative shear stress.

The B coefficient, which is proportional to the rotation of a yield surface with respect to (σ_{xx}, τ_{xy}) coordinate system, has no such simple physical interpretation as the coefficients described above and it cannot be deduced from uniaxial tests. In order to find its value it is necessary to carry out at least one test in a complex stress state.

The dimensions of the ellipse resulting from the considered yield condition for anisotropic materials are expressed in the form of functions of parameters of a second order curve, i.e.:

- coordinates of the ellipse centre:

$$\alpha_\sigma = \frac{BF - CD}{\delta}, \qquad \alpha_\tau = \frac{BD - AF}{\delta}, \tag{3.6}$$

- rotation angle of the ellipse axes with respect of (σ_{xx}, τ_{xy}) coordinate system:

$$\phi = \frac{1}{2} \arctan\left(\frac{2B}{A - C}\right), \tag{3.7}$$

- major (a) and minor (b) ellipse semi-axes:

$$a = \sqrt{-\frac{\Delta}{a'\delta}}, \qquad b = \sqrt{-\frac{\Delta}{b'\delta}}, \tag{3.8}$$

where

$$\Delta = -AC + 2BDF - CD^2 - AF^2 + B^2, \qquad \delta = AC - B^2 \tag{3.9}$$

and

$$\begin{aligned} a' &= \frac{1}{2}\left(A + C + \sqrt{(A - C)^2 + 4B^2}\right), \\ b' &= \frac{1}{2}\left(A + C - \sqrt{(A - C)^2 + 4B^2}\right). \end{aligned} \tag{3.10}$$

The coefficients of the ellipse equation, to fit the experimental data, are calculated by the least squares method. Such a procedure enables determination of all values of the ellipse coefficients in general form and, as a consequence, it provides information about the anisotropic properties of the tested material.

It is easy to show that other, often applied, yield conditions for anisotropic bodies result from Eq. (3.3). In order to obtain Hill's yield condition [40], one has to put $B = D = F = 0$ and so keeping the location of the centre and the axes unchanged. By putting $B = F = 0$, i.e. by making the major

axis of the ellipse (together with its centre) coincide with the σ_{xx} axis, the yield condition proposed by OTA *et al.* [44] is obtained.

The yield condition for anisotropic materials in the form (3.3) is determined by five material parameters. From a geometrical point of view they can be identified with the five ellipse parameters, i.e. its main axes, its center coordinates and its rotation angle with respect to the coordinate system.

4. EXPERIMENTAL RESULTS

4.1. Results for the material in the as-received state

Yield surfaces for the as-received 15 HM boiler steel obtained for the two different offsets $\varepsilon_{\text{off}} = 1 \times 10^{-5}$ and $\varepsilon_{\text{off}} = 5 \times 10^{-5}$ are shown in Fig. 7. Points in this figure represent experimental results while ellipses are determined by the least squares evaluation of the A, B, C, D, F coefficients in Eq. (3.3). Yield offset equal to 5×10^{-5} corresponds to the maximum value of the strain obtained in the yield surface determination tests. The other one is taken in order to study the shape and dimensions of the surfaces at the lower plastic deformation. It is seen that the material in the as-received state exhibits certain initial anisotropy reflected by the shift of the yield surface in the compression direction and in positive torsion direction as well. This anisotropy is presumably connected with the material texture induced due to the manufacture processes of the tubes used as the blanks for specimens.

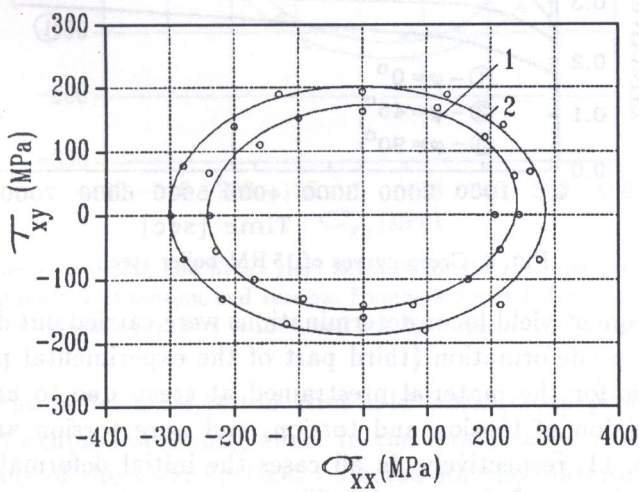

FIG. 7. Experimental points and fitted yield surfaces for the nondeformed (as-received) material. Numbers *1* and *2* denote results for the offsets equal to 1×10^{-5} and 5×10^{-5}, respectively.

4.2. Results for the material prestrained due to creep process

Creep curves for the boiler steel tested are presented in Fig. 8. They are representing material responses due to creep under uni-axial tension, combination of tension and torsion satisfying the condition $\varphi = \text{arctg}(\sqrt{3}\tau_{xy}/\sigma_{xx}) = 45°$, and pure torsion, all at the same effective stress equal to 370 [MPa]. It is clearly seen that the material exhibits anisotropy during creep process which is manifested by differences in strain rates and strain magnitudes measured at the end of tests. The greatest creep resistance of the steel tested in the considered time period was observed during tension test, while the lowest one at pure torsion. The difference in the strain amount obtained during creep tension and creep pure torsion referred to the strain level after creep tension exceeded 75 [%]. This result looks somewhat surprising with regard to the dimensions of the initial yield surface, since effective yield point obtained at pure torsion, 334 [MPa], was significantly higher than that at tension, 280 [MPa], for the yield offset 5×10^{-5}. Such material behaviour deals with the strain mechanisms controlling the deformation process, which are different for both prestraining processes taken into account.

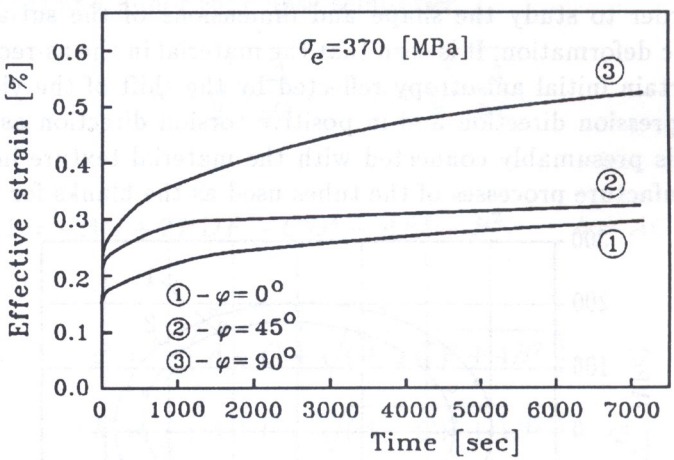

FIG. 8. Creep curves of 15 HM boiler steel.

The subsequent yield locus determinations were carried out directly after the testpiece predeformation (third part of the experimental programme). Yield surfaces for the material prestrained at creep due to uni-axial tension, combination of tension and torsion, and pure torsion are presented in Figs. 9, 10, 11, respectively. In all cases the initial deformation induced a strong anisotropy of the material. The greatest anisotropy was observed at directions coincident with predeformation paths. The magnitudes of the yield loci are shrunk in comparison to the initial yield surface, Fig. 7. It

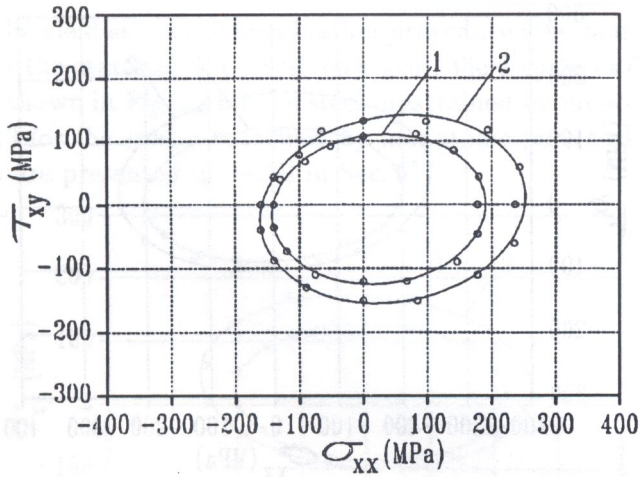

FIG. 9. Experimental points and fitted yield surfaces for the material prestrained due to creep at uni-axial tension. Numbers *1* and *2* denote results for the offsets equal to 1×10^{-5} and 5×10^{-5}, respectively.

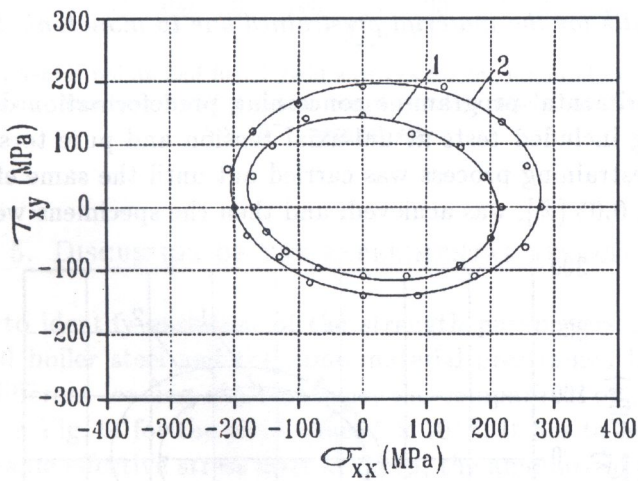

FIG. 10. Experimental points and fitted yield surfaces for the material prestrained due to creep at combination of tension and torsion. Numbers *1* and *2* denote results for the offsets equal to 1×10^{-5} and 5×10^{-5}, respectively.

means that the boiler steel tested after cold work (creep process at room temperature) exhibits softening effect in the strain range considered. The small rotations of the yield surfaces observed for the material prestrained by uni-axial tension and by pure torsion should be attributed to the history of previous probes made in order to determine the yield locus rather than to the predeformation induced by creep.

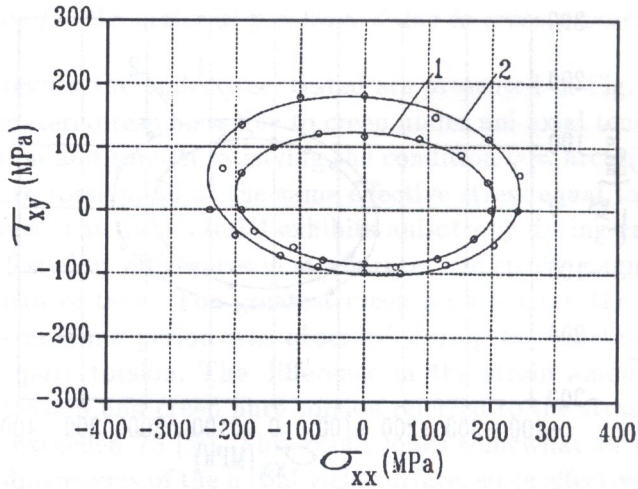

FIG. 11. Experimental points and fitted yield surfaces for the material prestrained due to creep at pure torsion. Numbers *1* and *2* denote results for the offsets equal to 1×10^{-5} and 5×10^{-5}, respectively.

4.3. Results for the material prestrained due to monotonic loading

The experimental programme concerning predeformation due to monotonic loading included tests at uni-axial tension and pure torsion. In both cases the prestraining process was carried out until the same effective total deformation, 0.65 [%], was achieved, and then the specimens were unloaded

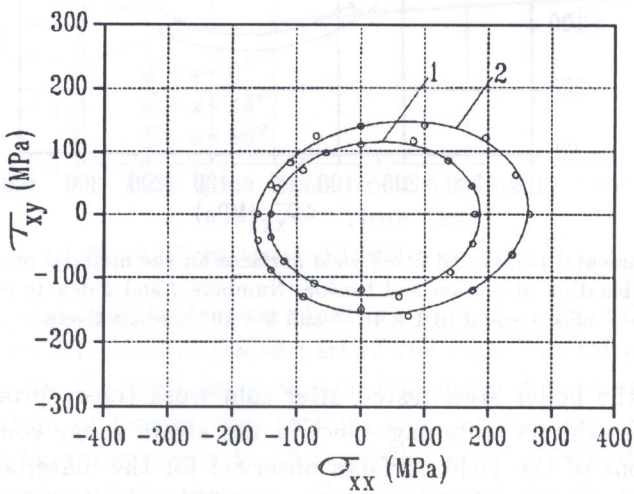

FIG. 12. Experimental points and fitted yield surfaces for the material prestrained due to monotonic tension. Numbers *1* and *2* denote results for the offsets equal to 1×10^{-5} and 5×10^{-5}, respectively.

followed by the yield surface determination procedure (the same as that used previously for the material in as-received state). Yield surfaces determined in this way are shown in Fig. 12 for the steel prestrained by monotonic tension, and in Fig. 13 for the steel prestrained by monotonic pure torsion. Study of these results are presented in detail in Sec. 5.

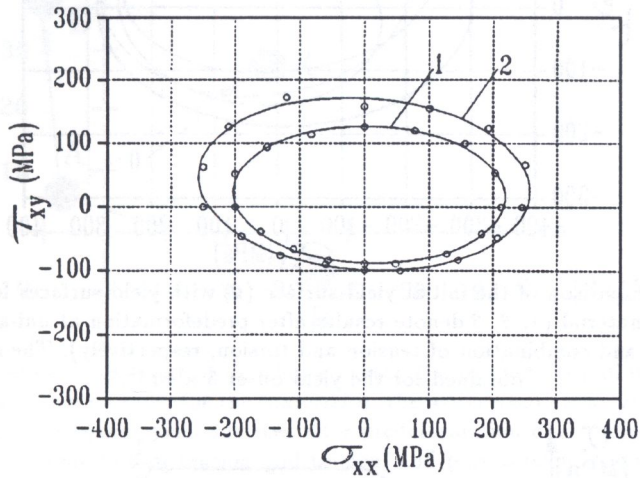

FIG. 13. Experimental points and fitted yield surfaces for the material prestrained due to monotonic torsion. Numbers *1* and *2* denote results for the offsets equal to 1×10^{-5} and 5×10^{-5}, respectively.

5. DISCUSSION OF THE EXPERIMENTAL RESULTS

In order to identify variation of the strength parameters for the as-received 15 HM boiler steel and the same material prestrained by creep process under different loading combinations, the comparison of yield surfaces is presented in Fig. 14 for the yield offset 5×10^{-5}. It has to be stated that despite the same effective stress level at creep, the amounts of prestrain are different depending on the stress state type. Hence, the comparison of the results in Fig. 14 can be treated as a first attempt to identify variations of the strength parameters due to creep prestraining. The differences achieved in the strain level are shown in Fig. 15 for all types of the constant loading processes performed. The monotonic loading path used to prestrain specimen either by uni-axial tension or pure torsion is also presented. However, in this case the total effective predeformation levels were the same, 0.65 [%]. It is easy to note, that the 15 HM boiler steel exhibits the softening effect due to the prior creep deformation at room temperature for all stress types taken into account, and is expressed by shrinking of dimensions of the yield

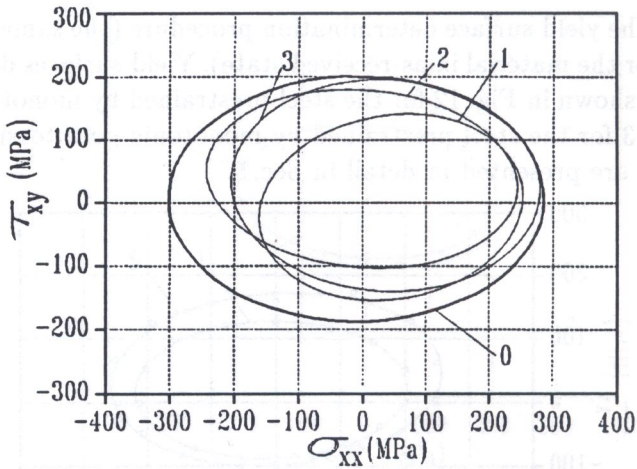

FIG. 14. Comparison of the initial yield surface (*0*) with yield surfaces for the creep prestrained material (*1, 2, 3* denote results after predeformation at uni-axial tension, pure torsion, and combination of tension and torsion, respectively). The surfaces were obtained for the yield offset 5×10^{-5}.

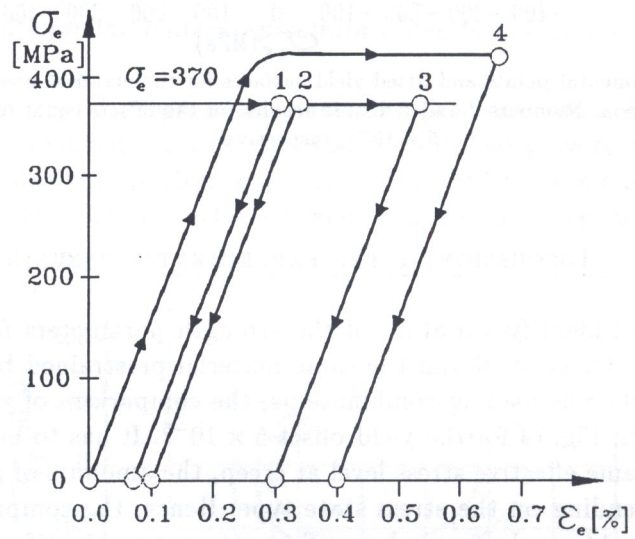

FIG. 15. Scheme of loading paths; constant loading used in creep processes (*1* – uni-axial tension, *2* – combination of tension and torsion, *3* – pure torsion), monotonic loading path (*4*) which was the same for tension and torsion loading processes in the $(\sigma_e, \varepsilon_e)$ plane.

surface. It has to be emphasized that the variations in effective prestraining level do not have essential influence on the effect observed. Analysis of locations of the yield loci shows shifts of the yield locus center in directions which are close to those used at the predeformation processes, Fig. 16.

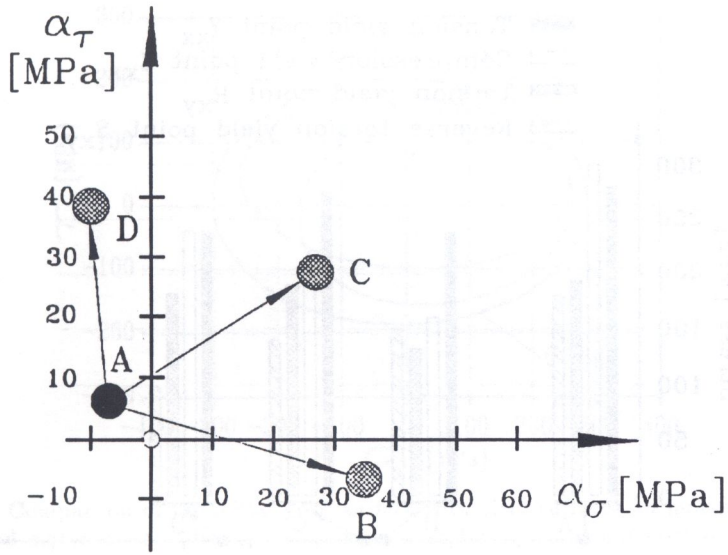

FIG. 16. Variation of the shift of the ellipse center due to predeformation; A denotes position of yield surface center for the material in the as-received state; B, C, D denote positions of the subsequent yield surfaces after predeformation due to creep at uniaxial tension, combination of tension and torsion, and pure torsion, respectively.

In order to make the anisotropy studies more visible, the values of yield limits for the four basic directions are graphically presented in Fig. 17. It contains the results for the material in the as-received state and the same material prestrained by creep at three different stress types for the same effective stress. It is shown that the non-deformed material demonstrated little anisotropy expressed in form of the differences of yield points between tension and compression (7 [%]) as well as between torsion and reverse torsion, also equal to 7 [%]. With regard to the prestrained material it is easy to note that the material softening effect is clearly reflected.

The Bauschinger effect is also well documented by the experimental results. The effect can be observed for the directions which are the same and reverse to those used at predeformation creep processes. In case of the creep-prestrained material due to uniaxial tension, the variation between yield points expressed as a ratio of the difference between tension and compression yield points referred to the tension yield limit equals 38 [%], while the similarly defined variation for the torsion and reverse torsion directions equals 8 [%]. Similar tendency can be observed for creep prestrained material due to pure torsion. The differences in yield limits for torsion and reverse torsion directions reached almost 45 [%] whereas yield limits obtained for tension and compression were the same.

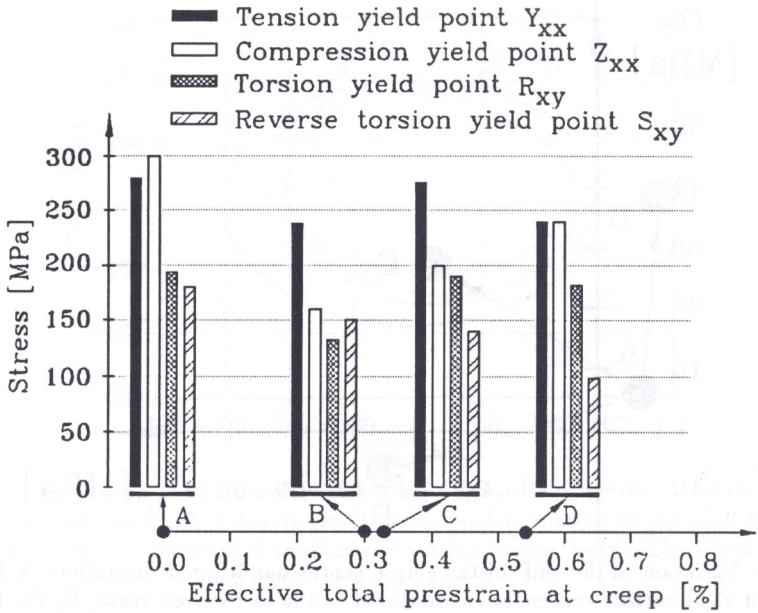

FIG. 17. Comparison of yield limits determined for the yield offset 5×10^{-5}; A denotes results for the non-deformed material, B denotes results for the material prestrained by creep at uni-axial tension, C denotes results for the material prestrained by creep at combination of tension and torsion, and D denotes results for the material prestrained by creep at pure torsion.

The same analysis has been carried out for the material prestrained by monotonic loading processes. The comparison of yield surfaces determined after this kind of plastic predeformation with the initial yield locus is presented in Fig. 18 for the offset strain equal to 5×10^{-5}. The steel tested after monotonic loading either at uniaxial tension or pure torsion possessed the remarkable softening effect in the strain region considered. Despite certain variations in the prestraining amount, the degree of softening does not essentialy differ for both prior cold work processes applied in the experimental programme. The same conclusion also deals with the other predeformation effects, e.g. translation of the initial yield surface center, Fig. 19, and the Bauschinger effect. Figure 20 illustrates the variations of yield limits due to the prestraining at both prior constant and monotonic loading processes. Besides the previously presented results for the as-received steel (A) and the same material after creep predeformation due to uni-axial tension (B) and pure torsion (C), Fig. 20 shows results for the material prestrained by means of monotonic loading at tension ($D1$) as well as at torsion ($D2$). Comparison of the experimental results for the same predeformation directions

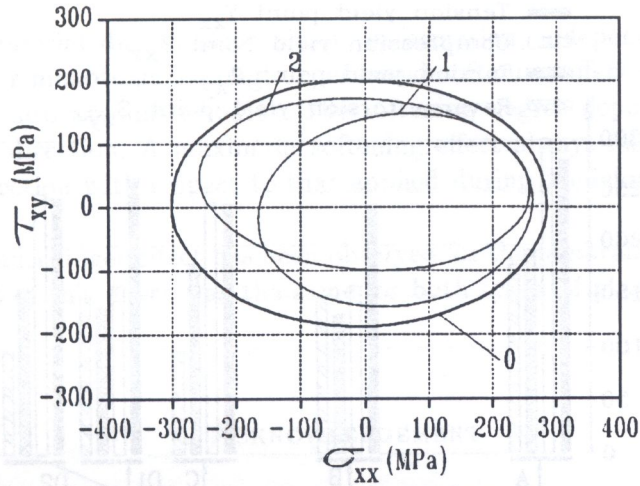

FIG. 18. Comparison of the initial yield surface with yield surfaces for monotonically prestrained material. (*1*, *2* denote results after predeformation at uni-axial tension, and pure torsion, respectively). The surfaces were obtained for the yield offset 5×10^{-5}.

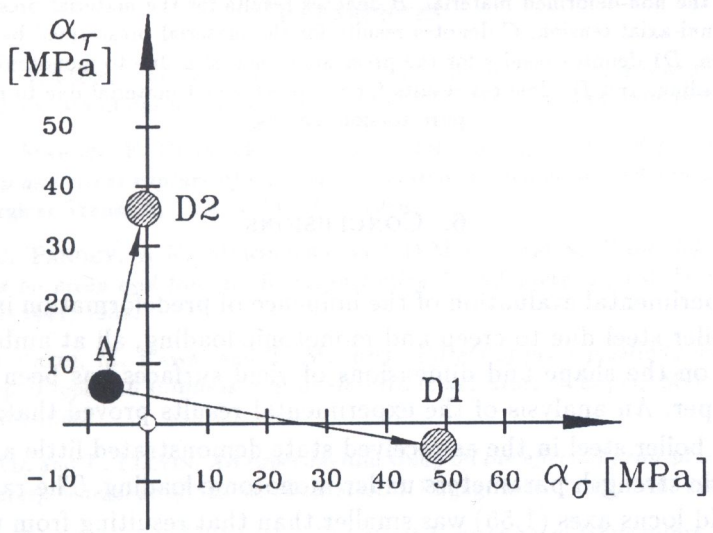

FIG. 19. Variation of the shift of the ellipse center due to monotonic predeformation; *A* denotes position of yield surface center for the material in the as-received state; *D*1, *D*2 denote positions of the subsequent yield surfaces after predeformation at uniaxial tension, and pure torsion, respectively.

obtained at different types of loading leads to the general remark that, in spite of some differences in the prestrain amount, the yield limits variations are almost the same (compare B with $D1$, and C with $D2$).

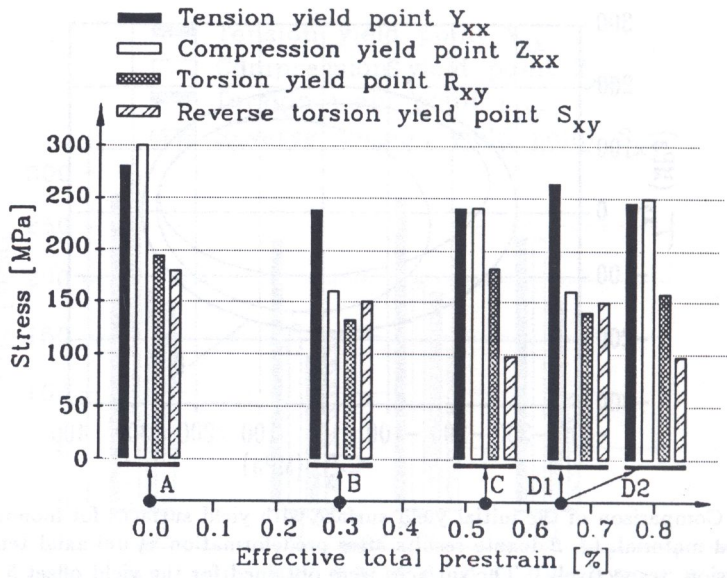

FIG. 20. Comparison of yield limits determined for the yield offset 5×10^{-5}; A denotes results for the non-deformed material, B denotes results for the material prestrained by creep at uni-axial tension, C denotes results for the material prestrained by creep at pure torsion, $D1$ denotes results for the prestrained material due to monotonic uni-axial tension loading, and $D2$ denotes results for the prestrained material due to monotonic pure torsion loading.

6. CONCLUSIONS

An experimental evaluation of the influence of predeformation induced in 15 HM boiler steel due to creep and monotonic loading, all at ambient temperature, on the shape and dimensions of yield surfaces has been reported in this paper. An analysis of the experimental results proved that:

1. The boiler steel in the as-received state demonstrated little anisotropy of the basic strength parameters under monotonic loading. The ratio of the initial yield locus axes (1.55) was smaller than that resulting from the Mises yield condition (1.73).

2. It has been found that the steel in the as-received state exhibited an anisotropy at creep loading conditions. This effect was manifested by the mutual location of creep curves determined for different types of stress states. The torsion constant loading path taken into account during creep tests was the weakest direction in the stress space considered, and this result differs from that obtained at monotonic loading where the torsion direction was the strongest one.

3. The material due to prior plastic deformation, independently of its type, creep or monotonic loading, experienced softening effect in the strain range taken into account (0.65%). The softening degree depended on the prestraining direction. A maximum softening effect always followed in the opposite direction with respect to that applied during predeformation process.

4. The Bauschinger effect has been observed for the prestrained material. The amount of this effect was the same for both types of plastic predeformation.

7. Acknowledgement

The author gratefully acknowledges the support of the Polish Committee of Scientific Research under grant No 3 0154 91 01.

References

1. R.N. Wilson, *The influence of 3% prestrain on the creep strength of Al-2.5% Cu-1.2% Mg alloys at 150 C*, J. Institute of Metals, **101**, 188–196, 1973.

2. R.T. Marlin, F. Cosandey and J.K. Tien, *The effect of predeformation on the creep and stress rupture of an oxide dispersion strengthened mechanical alloy*, Metallurgical Trans. A, **11A**, 1771–1775, 1980.

3. M.C. Pandey, A.K. Mukherjee and D.M.R. Taplin, *Prior deformation effects on creep and fracture in inconel alloy X-750*, Metallurgical Trans. A, **15A**, 1437–1441, 1984.

4. Y. Ohashi, M. Kawai and T. Momose, *Effects of prior plasticity on subsequent creep of type 316 stainless steel at elevated temperature*, J. Engng. Mat. Tech., **108**, 68–74, 1986.

5. Z. Xia and F. Ellyin, *An experimental study on the effect of prior plastic straining on creep behaviour of 304 stainless steel*, J. Engng. Mat. Tech., **115**, 200–203, 1993.

6. H.J. Tipler and R.K. Varma, *The effect of prior room temperature deformation on creep rupture and cavitation of 1/2Cr - 1/2Mo - 1/4V steels of commercial and high purity*, 3rd Int. Conf. Mech. Beh. Mat. Cambridge, 2, 321–329, 1979.

7. M. Waniewski, *The influence of direction and value of plastic prestrain on steady-state creep rate using the combined isotropic – kinematic hardening rule*, Engng. Trans., **32**, 523–535, 1984.

8. D.W.A. Rees, *Effects of plastic prestrain on the creep of aluminium under biaxial stress*, [in:] Creep and Fracture of Engineering Materials and Structures, B. Wilshire, D.R. Owen [Eds.], Proc. of Int. Conf., Swansea 1981, Pineridge Press, 559–572, 1981.

9. Z. KOWALEWSKI, *Creep behaviour of copper under plane stress state*, Int. J. Plasticity, **7**, 387–404, 1991.

10. Z. KOWALEWSKI, *The influence of deformation history on creep of pure copper*, [in:] Creep in Structures, Proc. 4th IUTAM Symp., Cracow 1990, M. ŻYCZKOWSKI [Ed.], Springer-Verlag, 115–122, 1991.

11. L. DIETRICH and Z.L. KOWALEWSKI, *Anisotropic properties development in copper subjected to plastic prestraining due to creep process and monotonic loading* [in Polish], IFTR Reports, 23, 1994.

12. W.A. TRĄMPCZYŃSKI, *The influence of cold work on the creep of copper under biaxial states of stress*, Acta Metall., **30**, 1035–1041, 1982.

13. W. SZCZEPIŃSKI, *On the effect of plastic deformation on yield condition*, Arch. Mech, **15**, 2, 275–296, 1963.

14. S.S. HECKER, *Experimental studies of yield phenomena in biaxially loaded metals*, [in:] Constitutive Equations in Viscoplasticity: Computational and Engineering Aspects, The Winter Annual Meeting of The American Society of Mechanical Engineers, New York City, NY, STRICKLIN and SACZALSKI [Eds.], ASME, AMD, 20, 1–33, 1976.

15. R. MARJANOVIC and W. SZCZEPIŃSKI, *Yield surfaces of the M-63 brass prestrained by cyclic biaxial loading*, Arch. Mech., **26**, 311–320, 1974.

16. J. MIASTKOWSKI, *Yield surface of material subjected to combined cyclic loading*, Arch. Mech., **30**, 203–215, 1978.

17. H. ISHIKAWA and K. SASAKI, *Stress-strain relations of SUS304 stainless steel after cyclic preloading*, J. Engng. Mat. Techn., **111**, 417–423, 1989.

18. H. ISHIKAWA and K. SASAKI, *Yield surfaces of SUS304 under cyclic loading*, J. Engng. Mat. Techn., **110**, 364–371, 1988.

19. J.F. WILLIAMS and N.L. SVENSSON, *Effect of tensile prestrain on the yield locus of 1100 - F aluminium*, J. Strain Anal., 5, 128–139, 1970.

20. Z.L. KOWALEWSKI, M. ŚLIWOWSKI and G. SOCHA, *Effect of cyclic prestrain orientation on yield surface evolution of 18G2A steel* [in Polish], IFTR Reports, 25, 1994.

21. L. DIETRICH, Z.L. KOWALEWSKI and M. ŚLIWOWSKI, *Anisotropy parameters variations of an aluminium alloy due to cyclic deformation* [in Polish], IFTR Reports, 27, 1994.

22. J.F. WILLIAMS and N.L. SVENSON, *Effect of torsional prestrain on the yield locus of 1100 - F aluminium*, J. Strain Anal., 6, 263–272, 1971.

23. J. MIASTKOWSKI and W. SZCZEPIŃSKI, *An experimental study of yield surfaces of prestrained brass*, Int. J. Solids and Struct., 1, 189–194, 1965.

24. W. SZCZEPIŃSKI, L. DIETRICH and J. MIASTKOWSKI, *Plastic properties of metals, Part 1*, [in:] Experimental Methods in Mechanics of Solids, PWN – Elsevier, 1990.

25. D.E. HELLING, A.K. MILLER and M.G. STOUT, *An experimental investigation of the yield loci of 1100-0 aluminum, 70:30 brass, and an overaged 2024 aluminum alloy after various prestrains*, J. Engng. Mat. Tech., **108**, 313–320, 1986.

26. M.R. WINSTONE and G.F. HARRISON, *Effects of overloads and creep on the yield surface of a nickel-based superalloy*, [in:] Techniques for Multi-Axial Creep Testing, D.J. GOOCH and I.M. HOW [Eds.], Elsevier Applied Science, London and New York 1986.

27. H.-C. WU and C.-C. HO, *Strain hardening of annealed 304 stainless steel by creep*, J. Engng. Mat. Tech., **115**, 345–350, 1993.

28. Y. OHASHI, M. KAWAI and H. SHIMIZU, *Effects of prior creep on subsequent plasticity of type 316 stainless steel at elevated temperature*, J. Engng. Mat. Tech., **105**, 257–263, 1983.

29. K. IKEGAMI and Y. NIITSU, *Effect of creep prestrain on subsequent plastic deformation*, Int. J. Plast., 1, 331–345, 1985.

30. K. IKEGAMI, *A historical perspective of the experimental study of subsequent yield surfaces for metal. Parts 1 and 2*, P. Soc. Mat. Sci., **4**, 491–505, 1975 and **24**, 709–719, 1975.

31. A. PHILLIPS, C.S. LIU and J.W. JUSTUSSON, *An experimental investigation of yield surfaces at elevated temperatures*, Acta Mech., **14**, 119–146, 1972.

32. E. SENDER, A. JARZĘBOWSKI and W. TRĄMPCZYŃSKI, *The theoretical prediction of the evolution of kinematic and isotropic hardening in the case of complex uniaxial loading*, [in:] Proc. Plasticity' 95, Dynamic Plasticity and Structural Behaviors, S. TANIMURA, A.S. KHAN [Eds.], Gorgon and Breach Publishers, Sakai, Japan, 645–648, 1995.

33. K. MALLICK, S.K. SAMANTA and A. KUMAR, *An experimental study of the evolution of yield loci for anisotropic materials subjected to finite shear deformation*, J. Engng. Mat. Tech., **113**, 192–198, 1991.

34. A. PHILLIPS, J.-L. TANG and M. RICCIUTI, *Some new observations on yield surfaces*, Acta Mech., **20**, 23–39, 1974.

35. A. PHILLIPS and J-L. TANG, *The effect of loading path on the yield surface at elevated temperatures*, Int. J. Solids Struct., **8**, 463–474, 1972.

36. E. SHIRATORI, K. IKEGAMI and K. KANEKO, *Plastic behaviours of initially anisotropic metals after multi-prestrainings*, [in:] Colloques Internationaux du CNRS No 295 - Comportement Mecanique Des Solides Anisotropes, 257–272.

37. W. SZCZEPIŃSKI, *On deformation-induced plastic anisotropy of sheet metals*, Arch. Mech., **45**, 1, 3–38, 1993.

38. B.F. DYSON and M.J. RODGERS, *Prestrain, cavitation and creep ductility*, Metal Sci., 8, 261, 1974.

39. B.F. DYSON, M.S. LOVEDAY and M.J. RODGERS, *Grain boundary cavitation under various states of applied stress*, Proc. R. Soc. London, Ser. **A 349**, 245, 1976.

40. R. HILL, *A theory of the yielding and plastic flow of anisotropic metals*, Proc. R. Soc. London, Ser. **A 193**, 281–297, 1948.

41. T.C. HSU, *Definition of the yield point in plasticity and its effect on the shape of the yield locus*, J. Strain Anal., **1**, 331–338, 1966.

42. R.V. MISES, *Mechanik der plastischen Formänderung von Kristallen*, Zeitsch. Angew. Math. Mech., **8**, 3, 161–185, 1928.

43. L. DIETRICH, R. KIRYK, G. SOCHA and M. ŚLIWOWSKI, *Identification of plastic anisotropy of an aluminium alloy* [in Polish], IFTR Reports, 26, 1994.

44. T. OTA, A. SHINDO and H. FUKUOKA, *A consideration on anisotropic yield criterion*, Proc. 9th Japan Nat. Cong. for Appl. Mech., 1959.

POLISH ACADEMY OF SCIENCES
INSTITUTE OF FUNDAMENTAL TECHNOLOGICAL RESEARCH.

Received October 9, 1995.